# Dynamic Reorganization of Vortex Matter into Partially Disordered Lattices

M. Marziali Bermúdez,[1,2] M. R. Eskildsen,[3] M. Bartkowiak,[4] G. Nagy,[5] V. Bekeris,[1,2] and G. Pasquini[1,2,*]
[1]Departamento de Física, Facultad de Ciencias Exactas y Naturales, Universidad de Buenos Aires, 1428 Buenos Aires, Argentina
[2]Instituto de Física de Buenos Aires, Consejo Nacional de Investigaciones Científicas y Técnicas, 1428 Buenos Aires, Argentina
[3]Department of Physics, University of Notre Dame, Notre Dame, Indiana 46556, USA
[4]Laboratory for Developments and Methods, Paul Scherrer Institut, CH-5232 Villigen, Switzerland
[5]Laboratory for Neutron Scattering and Imaging, Paul Scherrer Institut, CH-5232 Villigen, Switzerland
(Received 20 March 2015; published 4 August 2015; publisher error corrected 14 August 2015)

We report structural evidence of dynamic reorganization in vortex matter in clean $NbSe_2$ by joint small-angle neutron scattering and ac susceptibility measurements. The application of oscillatory forces in a transitional region near the order-disorder transition results in robust bulk vortex lattice configurations with an *intermediate* degree of disorder. These dynamically originated configurations correlate with intermediate pinning responses previously observed, resolving a long-standing debate regarding the origin of such responses.

DOI: 10.1103/PhysRevLett.115.067001 PACS numbers: 74.25.Uv, 61.05.fg, 64.60.Cn, 74.81.Bd

In a wide variety of complex systems, competing interactions promote an order-disorder transition (ODT). Ordered phases are characterized by spatial correlations decaying weakly over distances larger than the relevant system scale, whereas disordered configurations are characterized by correlation lengths $\zeta$ of the order of the mean interparticle distance $a_0$. Configurations with intermediate degrees of disorder, strong enough to affect the system response, but still with $\zeta \gg a_0$, have received attention recently [1]. Vortex matter in superconductors provides an ideal model system for the experimental study of the topic [2]: vortex-vortex interactions favoring an ordered vortex lattice (VL) compete with both thermal fluctuations and pinning interactions that tend to disorder the system.

In very low-pinning superconductors, such as clean $NbSe_2$ single crystals, most of the vortex field-temperature phase diagram is properly described by an ordered dislocation-free Bragg glass (BG) phase [3–5], which undergoes an ODT near the normal-superconductor transition [6–8]. In practice, when a superconductor is cooled from the normal state in an external magnetic field [field-cooled (FC)], energy barriers may trap the VL in highly disordered metastable configurations [8]. Even so, high transport current densities [9,10] or large oscillatory "shaking" magnetic fields [11,12] may anneal the VL into the ordered low-temperature BG. Once in the BG, as temperature or magnetic field is increased, the VL softens and accommodates to the random pinning potential more efficiently. Eventually, vortex entanglement and the proliferation of VL dislocations increase the effective pinning, producing a sudden rise of the critical current $J_c$ known as the peak effect (PE) [7,8], which is the fingerprint of the ODT in vortex matter. While both the high-pinning disordered phase and the low-pinning ordered phase, above and below the ODT, are widely accepted in the literature, intermediate responses have been ascribed to surface contamination and partial reordering by the probing transport current [9,10,13,14]. However, in the narrow transitional region adjacent to the PE, for which a multidomain phase has been theoretically proposed [15], noninvasive techniques have shown that pinning can be *partially decreased* or even *increased* by applying dc currents [16,17] or ac magnetic fields [11]. The resulting intermediate responses are highly reproducible and independent of the previous history. Are these in-between responses originated from bulk VL configurations with an intermediate degree of disorder?

To address this question, we performed an experiment in a clean $NbSe_2$ single crystal, combining small-angle neutron scattering (SANS) with *in situ* linear ac susceptibility measurements. In SANS imaging of a perfect triangular VL, first order Bragg peaks (BP) are expected to appear as six symmetric sharp spots, matching the reciprocal lattice vectors. This still holds for an ideal BG, where elastic disorder leads to slow decay of the correlations [4], although recent simulations [18] have shown that elastic BG prefracturing would result in a slight broadening of the BPs. Conversely, when disorder is dominated by dislocations, spatial correlations decay exponentially beyond a characteristic length $\zeta$ associated with the scale at which dislocations appear [19]. In such cases BPs have a finite intrinsic width proportional to $\zeta^{-1}$. Experimentally observed BPs are further smeared by a convolution kernel due to finite resolution [20]. Hence, the degree of disorder can be determined from the spread of the scattered intensity, as long as $\zeta \lesssim L_{\mathrm{res}}$, a resolution-dependent bound. In a 3D vortex system, the anisotropy of the elastic constants gives rise to very different characteristic lengths along the direction of the flux lines ($\zeta_L$) and in the transverse plane ($\zeta_\perp$). Because of the poorer in-plane resolution, in this experiment only the longitudinal $\zeta_L$

 

was determined by measuring the integrated intensity on the plane of a single BP as the sample was rocked through the Bragg condition [rocking curve (RC)].

The experiment was conducted at the SANS-II beam line of the Paul Scherrer Institute's SINQ facility, using the MA11 cryomagnet. The geometry of the experiment is sketched in Fig. 1. All SANS measurements were performed at $T_0 = 1.9$ K. The neutron wavelength was chosen to be $\lambda_N \approx 9$ Å ($\pm 10\%$) and the applied dc field was $H = 5$ kOe. The incident beam was collimated, resulting in a beam divergence $\sim \pm 0.05°$. The angular resolution along the rocking angle was estimated to be $w_{\rm res} = (0.107° \pm 0.004°)$. A statistical analysis showed that curves arising from $\zeta_L < L_{\rm res} \sim 40$ $\mu$m were distinguishable from the resolution kernel. RCs wider than our resolution were fitted by the convolution of the Gaussian resolution with a Lorentzian distribution corresponding to an intrinsic $\Delta q_L = 2/\zeta_L$ [21]. A large ($5.6 \times 4.7 \times 0.2$ mm$^3$) clean $NbSe_2$ single crystal was used for the experiment. The sample is part of a batch grown in Bell Labs as described in Ref. [27], with $T_c = (7.115 \pm 0.029)$ K (10%–90% of the linear ac susceptibility transition at $H = 0$). The phase diagram for various crystals has been built using a 7-T MPMS XL (Quantum Design) and compared with those published in the literature [17], showing nonsignificant differences [21].

Since the goal was to explore the connection between structure and dynamics, a noninvasive measurement of pinning was required. This was achieved by installing a sample holder with mutual inductance coils inside the SANS cryomagnet. By adding a small ac magnetic field $h_{\rm ac} = 2.5$ mOe ($< 10^{-6} H, f = 65$ kHz), vortices were forced to perform small oscillations inside their pinning wells, without modifying their spatial configuration. These oscillations propagate through the sample due to the vortex-vortex repulsion, with a characteristic penetration depth $\lambda_{\rm ac}$ that is related, in a mean-field approximation [28], to the effective pinning potential [29]. The linearity of the response, as well as the low dissipation level characteristic of the linear Campbell response [29] had been previously verified. Then $\lambda_{\rm ac}$ and thus the effective pinning can be assessed through the in-phase component of the linear ac susceptibility $\chi'$ by means of a mutual inductance technique. Lower values of $\chi'$ are associated with stronger pinning, saturating at perfect ac shielding (normalized to $\chi' = -1/4\pi$), whereas $\chi'$ vanishes under complete ac penetration when $\lambda_{\rm ac} \gtrsim$ sample size. To probe oscillatory dynamic effects, a shaking procedure was applied at certain temperatures: Here $\chi'$ measurements were paused and a larger sinusoidal field with amplitude $h_{\rm sh} = 7$ Oe, and $f_{\rm sh} = 1$ kHz was applied for 1000 cycles before returning to the smaller $h_{\rm ac}$ to resume $\chi'$ measurements. The shaking field amplitude was sufficient to induce vortex displacements larger than $a_0$ throughout the sample. The complete penetration of the shaking field into the sample had been previously confirmed by measuring the nonlinear ac response and checking consistency with the irreversible dc magnetization determined from $M(H)$ loops [21].

Figure 2(a) shows a comparison between $\chi'(T)$ measured during a FC procedure and after shaking the VL at two different temperatures $T_{\rm sh}^{(1,2)}$ below the onset of the PE at $T_{\rm po} \simeq 6.27$ K. There is an unambiguous rise in $\lambda_{\rm ac}$ after shaking, representing a reduction of the effective pinning. The agreement between both cooling $\chi'(T)$ curves after shaking is consistent with an equilibration procedure below

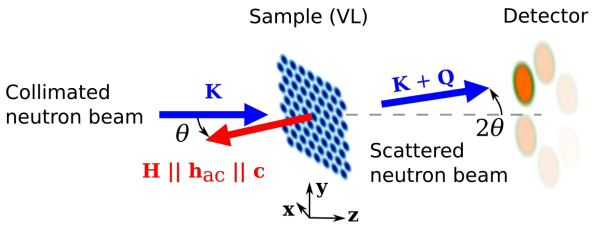


FIG. 1 (color online). Scattering geometry: Both the dc field **H** and the ac field $\mathbf{h}_{\rm ac}$ are aligned with the **c** axis of the single crystal, in the **xz** plane. As the whole system is *rocked* around the **y** axis, the distribution of the scattered intensity $I$ is measured by the position-sensitive detector, which spans the **xy** plane, for each angle $\theta$ between the field direction and incoming neutron beam wave vector **K**. The maximum intensity is expected at $\theta_0 = Q_0/K$, for the corresponding reciprocal lattice vector $\mathbf{Q}_0$.

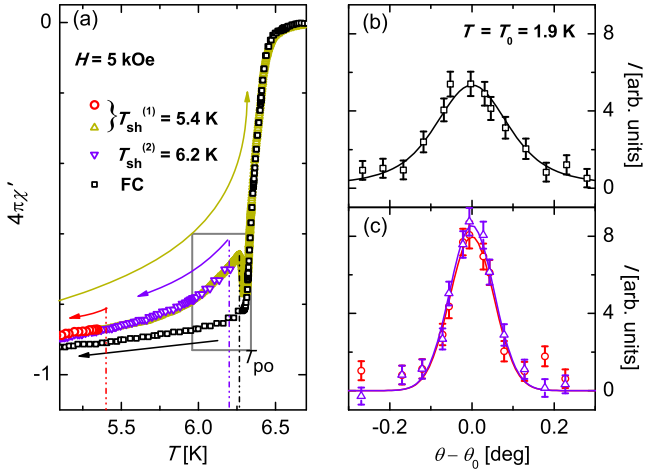


FIG. 2 (color online). (a) Linear ac susceptibility $\chi'(T)$ measured down to $T_0 = 1.9$ K during a FC cooling procedure (black squares) and after shaking the VL at two different temperatures $T_{\rm sh}^{(1,2)}$ (red circles and violet triangles) below the onset of the PE ($T_{\rm po}$). Shaking temperatures are indicated by vertical lines and arrows indicate temperature evolution. Reversibility is observed in the warming from $T_0$ of the VL shaken at $T_{\rm sh}^{(1)}$ (dark yellow triangles). The area enclosed by the rectangular box is magnified in Fig. 3(a). (b) RC after FC; the black curve is the fit of a Lorentzian peak convoluted by the resolution kernel. (c) RCs after shaking the VL at $T_{\rm sh}^{(1)}$ (red circles) and $T_{\rm sh}^{(2)}$ (violet triangles); the curves are Gaussian fits with FWHM equal to the instrumental resolution $w_{\rm res} = 0.107°$.

$T_{po}$. Reversibility is observed in the warming curve, with $\chi'(T)$ increasing with $T$ up to $T_{po}$, after which it drops due to the spontaneous pinning enhancement at the PE. In contrast, the absence of PE in the linear response during the cooling [11] is likely due to the VL remaining trapped in a metastable highly pinned state. This explanation is consistent with the FC RC [Fig. 2(b)], which is clearly wider than the resolution kernel, in agreement with other experiments [30,31]. Conversely, the two RCs recorded after shaking the VL [Fig. 2(c)] show resolution-limited BPs ($\zeta_L > L_{res}$). The fact that BPs are well defined (unlike the annulus observed for amorphous VLs) indicates that orientational order is preserved in all the cases. The broadening of the FC configuration RC suggests a dislocated VL with broken positional order beyond a characteristic volume with longitudinal dimension $\zeta_L < L_{res}$. There is a clear correlation between the ordering of the VL and the decrease of the effective pinning.

While shaking the VL at any $T_{sh} < T_{po}$ leads to an ordered configuration, the consequences are strikingly different when the shaking field is applied in the narrow transitional region above $T_{po}$. Figure 3(a) shows the evolution of $\chi'(T)$ through a series of processes near the transitional region (hatched area) and Fig. 4(a) displays the corresponding RCs. A strongly pinned FC VL was cooled to $T_{sh}^{(3)} = 6.29\text{K} > T_{po}$ and shaken, partially reducing the effective pinning. The VL was cooled to $T_0$ and a narrow RC, still wider than $w_{res}$ was measured, indicating a bulk *partial ordering*. In contrast, applying the same shaking burst at the same $T_{sh}^{(3)}$ ($\pm 3$ mK) to an initially ordered VL had the opposite effect: The shaking field partially increased the effective pinning to a similar level and *disordered* the VL. The RC was broader than $w_{res}$, but narrower than for the maximally disordered FC lattice. Because the response after shaking is strongly dependent on the temperature when $T_{sh} > T_{po}$, the process was carefully repeated within $\Delta T_{sh} \sim 3$ mK, obtaining the same

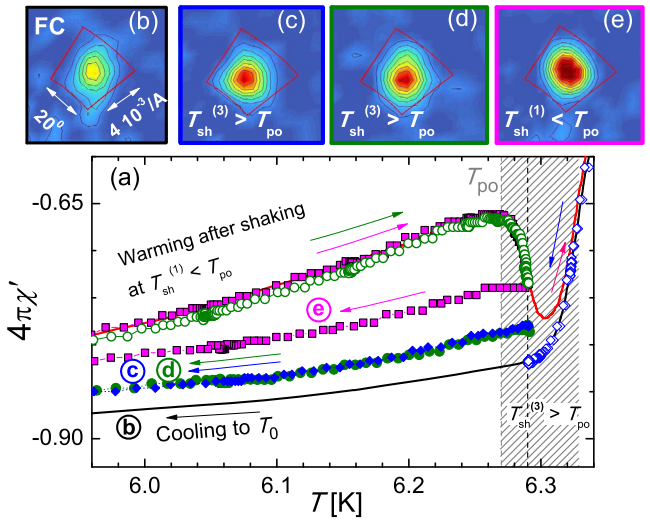


FIG. 3 (color online). $\chi'(T)$ for different thermal and dynamic histories [labeled (b)–(e) in panel (a)] and the corresponding detector intensity distributions for one VL BP at the Bragg condition [panels (b)–(e)]. Arrows in (a) indicate temperature evolution and the hatched area shows the transitional region. Data from Fig. 2(a) (black and red lines) is included for comparison. The application of a shaking field at $T_{sh}^{(3)} \cong 6.29$ K $> T_{po}$ results in a unique response (full blue and green symbols) independent of whether the initial state was a disordered FC VL (open blue symbols) or an ordered VL (open green symbols). Both intensity distributions (c) and (d) indicate partial disorder as compared to the FC intensity distribution (b). Simply warming an ordered VL (magenta squares) up to $T \cong T_{sh}^{(3)}$ shows moderate pinning enhancement during cooling, but the corresponding BP (e) is still sharp and intense. The red boxes in (b)–(e) enclose the detector area included in the RCs in Fig. 4.

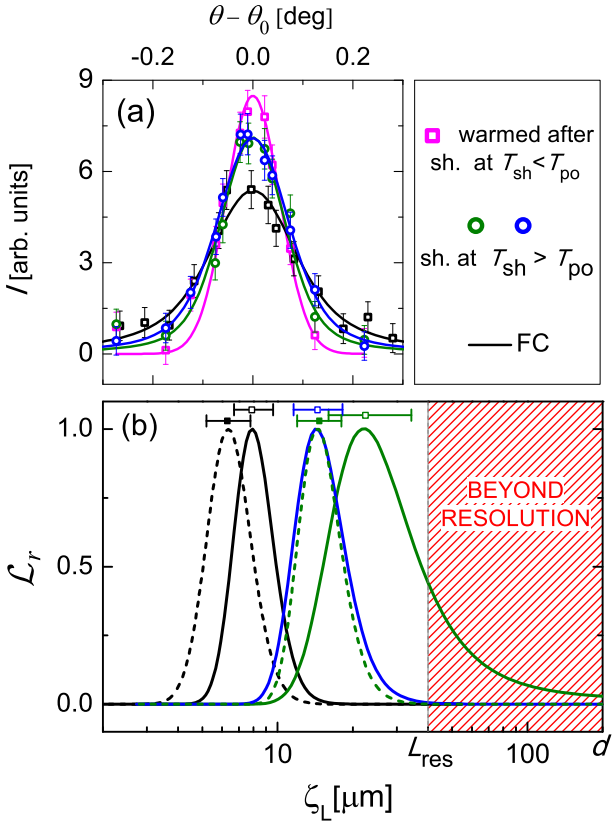


FIG. 4 (color online). (a) Rocking curves measured after different field-temperature histories: FC [black, same as in Fig. 2(b)], after shaking at $T_{sh}^{(3)}$ a FC (blue) and an ordered (green) VL, and after warming an ordered VL to $T = T_{sh}^{(3)}$ without shaking at this temperature (magenta). Curves are fits of Lorentzian peaks convoluted by the resolution. (b) Calculated profile likelihood ratio $\mathcal{L}_r$ as a function of $\zeta_L$ up to the sample thickness $d$ for each experimental RC. Symbols above the curves indicate the maximum ($\mathcal{L}_r \equiv 1$) and error bars, the 68% confidence interval. For the ordered VL, $\zeta_L > L_{res} \sim 40\ \mu\text{m} \sim 570 a_0$ and is beyond our resolution. The profile likelihood of replicate RCs of the FC (black dashed line) and the one shaken at $T_{sh}^{(3)} \pm 3$ mK (green dashed line) are reproducible within the error bars.

qualitative results. To rule out that the partial disordering was of thermal origin, a warming-cooling cycle up to $T_{sh}^{(3)}$, but without applying the shaking burst, was carried out for a replicated ordered VL. Although the cooling $\chi'(T)$ branch indicates higher pinning than the warming branch, it is lower than for VLs shaken above $T_{po}$. Moreover, if there was any associated disorder, it was minor and below our SANS resolution. Therefore, the "intermediate" degree of disorder found before is only attributable to the shaking field applied at $T_{sh}^{(3)}$.

Although the above results are qualitatively evident by simply comparing the corresponding intensity distribution on the position-sensitive detector at $\theta = \theta_0$ [Fig. 3(b)–(e)], we evaluated the statistical significance of the observed differences [21]. Figure 4(b) shows the profile likelihood ratio $\mathcal{L}_r(\zeta_L)$ resulting from the fit of each experimental RC to one expected from a configuration with an intrinsic width given by $\zeta_L$ convoluted by the experimental resolution. Correlation lengths obtained after shaking the VL at $T_{sh}^{(3)}$ were $L_{res} > \zeta_L > \zeta_L(\mathrm{FC})$ at the 75% confidence level. Thus, we state that shaking the VL in the transitional region results in bulk intrinsic configurations with an intermediate degree of disorder.

The total integrated intensity $I_0$ (the area under the RC) for the different configurations should remain roughly constant. Even so, the long-tail decay of the structure factor in the BG phase may lead to an underestimation of $I_0$ [4]. Indeed, for all FC configurations and for the configurations obtained after shaking the VL in the transitional region we observe a similar $I_0$. However, for the lattice shaken in the BG the integrated intensity is slightly, but statistically significant, smaller [21]. These features support a qualitative difference in the positional order decay in the elastic BG configurations and in those obtained after shaking the VL in the transitional region, where disorder is probably mediated by dislocations.

In the elastic BG, the in-plane correlation length $\zeta_\perp$ can be derived from $\zeta_L$ through the tilt and shear elastic constants $c_{44}$ and $c_{66}$ [3,4,32,33]. From $L_{res}$, a lower limit of $35a_0$ can be estimated for the in plane size of the dislocation-free regions corresponding to the ordered configurations, which is consistent with results obtained in other works in the BG phase [4,30,34]. How $\zeta_\perp$ relates to $\zeta_L$ is not as straightforward for metastable VL configurations with dislocations. In theoretical works [35,36], $\zeta_L$ and $\zeta_\perp$ are obtained for equilibrium VL configurations from the densities of screw and edge dislocations that minimize the free energy; far enough from the amorphous limit (i.e., $\zeta_\perp \sim a_0$) dislocation densities adapt in such a way as to satisfy the elastic ratio. Moreover, numerical simulations [37] and experimental results [38] show that $\zeta_L$ monotonically increases with the in-plane ordering from the plastic to the elastic regime. In our case, the partially disordered VLs are metastable configurations (at $T_0$) which originated from a dynamic reorganization in the vicinity of the ODT. In this region the elastic constants are dispersive and may also be affected by fluctuations. Therefore, a precise quantitative estimation of $\zeta_\perp$ from $\zeta_L$ is not available, but a monotonic correlation is still expected (see Ref. [21] for a quantitative estimate). Such a correlation would be compatible with an intermediate density of dislocations in partially disordered VLs.

Our results show a clear connection between the linear ac response, related to the effective pinning, and the bulk spatial correlation of the VL. Configurations having correlation lengths much larger than the lattice parameter, but small enough to affect the global response, were observed after shaking the VL in the proposed transitional region. These observations support the existence of such a region and represent the first evidence of a dynamic reordering, driven by oscillatory forces, which results in robust bulk configurations with intermediate degrees of disorder. A similar behavior was obtained in numerical simulations [12], where configurations with intermediate dislocation densities are accessible from stationary fluctuating dynamic states, as those proposed for colloids [39,40]. The interplay between these spatial configurations and their associated nonlinear dynamics remains a fertile ground for further research.

This work is based on experiments performed at the Swiss spallation neutron source SINQ, Paul Scherrer Institute, Villigen, Switzerland, and was partially supported by ANPCyT under Grant PICT No. 753 and CONICET under Grant PIP 536. M. R. E. was supported by the U.S. Department of Energy, Basic Energy Sciences under Award No. DE-FG02-10ER46783. We are grateful to G. Nieva for providing the $NbSe_2$ sample, Fundación Juan Bautista Sauberán, Universidad de Buenos Aires and M. Kenzelmann for financial aid, and E. R. De Waard for assistance with the SANS experiment.

*pasquini@df.uba.ar

[1] C. P. Goodrich, A. J. Liu, and S. R. Nagel, Nat. Phys. **10**, 578 (2014).
[2] I. Guillamón, R. Córdoba, J. Sesé, J. M. De Teresa, M. R. Ibarra, S. Vieria, and H. Suderow, Nat. Phys. **10**, 851 (2014).
[3] T. Giamarchi and P. Le Doussal, Phys. Rev. B **52**, 1242 (1995).
[4] T. Klein, I. Joumard, S. Blanchard, J. Marcus, R. Cubitt, T Giamarchi, and P. Le Doussal, Nature (London) **413**, 404 (2001).
[5] X. Du, G. Li, E. Y. Andrei, M. Greenblatt, and P. Shuk, Nat. Phys. **3**, 111 (2007).
[6] T. Giamarchi and P. Le Doussal, Phys. Rev. B **55**, 6577 (1997).
[7] A. M. Troyanovski, M. van Hecke, N. Saha, J. Aarts, and P. H. Kes, Phys. Rev. Lett. **89**, 147006 (2002).
[8] P. L. Gammel, U. Yaron, A. P. Ramirez, D. J. Bishop, A. M. Chang, R. Ruel, L. N. Pfeiffer, E. Bucher, G. D'Anna,

D. A. Huse, K. Mortensen, M. R. Eskildsen, and P. H. Kes, Phys. Rev. Lett. **80**, 833 (1998).
[9] W. Henderson, E. Y. Andrei, M. J. Higgins, and S. Bhattacharya, Phys. Rev. Lett. **77**, 2077 (1996).
[10] Y. Paltiel, E. Zeldov, Y. N. Myasoedov, H. Shtrikman, S. Bhattacharya, M. J. Higgins, Z. L. Xiao, E. Y. Andrei, P. L. Gammel, and D. J. Bishop, Nature (London) **403**, 398 (2000).
[11] G. Pasquini, D. Pérez Daroca, C. Chiliotte, G. S. Lozano, and V. Bekeris, Phys. Rev. Lett. **100**, 247003 (2008).
[12] D. Pérez Daroca, G. Pasquini, G. S. Lozano, and V. Bekeris, Phys. Rev. B **84**, 012508 (2011).
[13] H. A. Hanson, X. Wang, I. K. Dimitrov, J. Shi, X. S. Ling, B. B. Maranville, C. F. Majkrzak, M. Laver, U. Keiderling, and M. Russina, Phys. Rev. B **84**, 014506 (2011).
[14] A. Pautrat, M. Aburas, Ch. Simon, P. Mathieu, A. Brûlet, C. D. Dewhurst, S. Bhattacharya, and M. J. Higgins, Phys. Rev. B **79**, 184511 (2009).
[15] G. I. Menon, Phys. Rev. B **65**, 104527 (2002); G. I. Menon, G. Ravikumar, M. J. Higgins, and S. Bhattacharya, Phys. Rev. B **85**, 064515 (2012).
[16] Z. L. Xiao, E. Y. Andrei, P. Shuk, and M. Greenblatt, Phys. Rev. Lett. **85**, 3265 (2000).
[17] Z. L. Xiao, O. Dogru, E. Y. Andrei, P. Shuk, and M. Greenblatt, Phys. Rev. Lett. **92**, 227004 (2004).
[18] M. Laver, E. M. Forgan, A. B. Abrahamsen, C. Bowell, Th. Geue, and R. Cubitt, Phys. Rev. Lett. **100**, 107001 (2008).
[19] T. Giamarchi and P. Le Doussal, Phys. Rev. Lett. **75**, 3372 (1995).
[20] M. R. Eskildsen, Front. Phys. **6**, 398 (2011).
[21] See Supplemental Material at http://link.aps.org/supplemental/10.1103/PhysRevLett.115.067001, which includes Refs. [22–26], for details about the statistical analysis of SANS data and magnetization measurements, as well as a discussion on the relationship between $\zeta_L$ and $\zeta_\perp$.
[22] C. Dewhurst, computer code GRASP: Graphical Reduction and Analysis SANS Program, version 6.93b, 2014.
[23] J. W. Eaton, D. Bateman, and S. Hauberg, *GNU Octave Version 3.0.1 Manual: A High-Level Interactive Language for Numerical Computations* (CreateSpace, 2009).
[24] M. R. Eskildsen, Ph.D. thesis, Risø National Laboratory and University of Copenhagen, Denmark, 1998.
[25] J. R. Clem and A. Sanchez, Phys. Rev. B **50**, 9355 (1994).
[26] E. H. Brandt, Phys. Rev. B **60**, 11939 (1999).
[27] C. S. Oglesby, E. Bucher, C. Kloc, and H. Hohl, J. Cryst. Growth **137**, 289 (1994).
[28] B. Raes, C. C. de Souza Silva, A. V. Silhanek, L. R. E. Cabral, V. V. Moshchalkov, and J. Van de Vondel, Phys. Rev. B **90**, 134508 (2014).
[29] A. M. Campbell, J. Phys. C **4**, 3186 (1971).
[30] U. Yaron, P. L. Gammel, D. A. Huse, R. N. Kleiman, C. S. Oglesby, E. Bucher, B. Batlogg, D. J. Bishop, K. Mortensen, and K. N. Clausen, Nature (London) **376**, 753 (1995).
[31] N. D. Daniilidis, S. R. Park, I. K. Dimitrov, J. W. Lynn, and X. S. Ling, Phys. Rev. Lett. **99**, 147007 (2007).
[32] $\lambda(T)$ has been estimated from J. D. Fletcher, A. Carrington, P. Diener, P. Rodiére, J. P. Brison, R. Prozorov, T. Olheiser, and R. W. Giannetta, Phys. Rev. Lett. **98**, 057003 (2007).
[33] E. H. Brandt, Rep. Prog. Phys. **58**, 1465 (1995).
[34] S. C. Ganguli, H. Singh, G. Saraswat, R. Ganguly, V. Bagwe, P. Shirage, A. Thamizhavel, and P. Raychaudhuri, Sci. Rep. **5**, 10613 (2015).
[35] S. J. Mullock and J. E. Evetts, J. Appl. Phys. **57**, 2588 (1985).
[36] M. C. Marchetti and D. R. Nelson, Phys. Rev. B **41**, 1910 (1990); J. Kierfeld and V. Vinokur, Phys. Rev. B **61**, R14928 (2000).
[37] A. B. Kolton, D. Domínguez, C. J. Olson, and N. Grønbech-Jensen, Phys. Rev. B **62**, R14657 (2000).
[38] U. Yaron, P. L. Gammel, D. A. Huse, R. N. Kleiman, C. S. Oglesby, E. Bucher, B. Batlogg, D. J. Bishop, K. Mortensen, K. Clausen, C. A. Bolle, and F. De La Cruz, Phys. Rev. Lett. **73**, 2748 (1994).
[39] L. Corté, P. M. Chaikin, J. P. Gollub, and D. J. Pine, Nat. Phys. **4**, 420 (2008).
[40] C. Reichhardt and C. J. Olson Reichhardt, Phys. Rev. Lett. **103**, 168301 (2009).